

Epitaxial growth of silicon: A molecular-dynamics simulation

M. Schneider and Ivan K. Schuller

Materials Science Division, Argonne National Laboratory, Argonne, Illinois 60439

A. Rahman*

Supercomputer Institute, School of Physics and Astronomy,
University of Minnesota, Minneapolis, Minnesota 55455

(Received 5 December 1986)

We have studied the epitaxial growth of silicon using molecular-dynamics techniques. The model consists of a temperature-controlled Si(111) substrate, with the Si atoms projected towards the substrate as is done in the laboratory. The atoms interact via a potential developed by Stillinger and Weber to simulate the bulk properties of Si. We find that at low substrate temperatures the growth is not well ordered; this is in accordance with experimental observation. It is precisely the opposite of what occurs in spherically symmetric potentials that were used to simulate the growth of metallic films. At higher substrate temperatures the growth is into properly stacked, crystalline Si layers. In contrast to the growth of metals (spherically symmetric potentials), the atomic mobility on the growing surface and the thermal conductivity of the system are much lower for Si; the results of this simulation and those of our previous work are in agreement with experimental observations showing, as expected, that a major determining factor in epitaxial growth of films is the nature of the interaction potential.

Epitaxial growth from the vapor phase is a subject of much current interest.¹ This is motivated by the unique physics and materials which can be studied using this technique, and by important applications in the fields of semiconductors, magnetism, and optics. The theoretical studies to date have mostly been based on phenomenological, thermodynamic models which rely on a variety of parameters whose significance, quantitative and qualitative, is unknown *a priori*.² Recent advances in computer technology have opened up the possibility for realistic simulations of epitaxial processes.³⁻⁵ These simulations are useful in understanding the role of the various parameters important for epitaxial growth. We present here the first molecular-dynamics (MD) simulation of epitaxial growth of silicon on a Si(111) substrate. At very low substrate temperatures the growth is found to be in a disordered structure. Our results show that there is an optimum range of temperatures for which epitaxial growth occurs, and that dynamical relaxation is an essential factor in this process. However, the surface mobility for the case of fourfold-coordinated elements such as silicon is much smaller than the one found for spherically symmetric potentials. We speculate that in the laboratory this is the reason for the easier epitaxial growth of metals as compared to semiconductors and that the interfaces might be sharper in semiconducting than in metallic superlattices.

In the calculation presented here the atoms interact via a potential developed by Stillinger and Weber⁶ (SW) to simulate the properties of liquid and solid silicon. The potential comprises both two-body and three-body contributions. The two-body part has a Lennard-Jones-type form

$$f_2(r_{ij}) = A(Br_{ij}^{-p} - 1) \exp[(r_{ij} - a)^{-1}], \quad (1)$$

with $A = 7.049\,556$, $B = 0.602\,224\,6$, $p = 4$, $a = 1.80$. The minimum of f_2 is at $r_{\min} = 2^{1/6}$ with a depth

$f_2(r_{\min}) = -1$. The three-body part of the potential energy consists of a sum of the following term over all triplets:

$$f_3(r_{ij}, r_{ik}, \theta_{jik}) = \lambda \exp[\gamma(r_{ij} - a)^{-1} + \gamma(r_{ik} - a)^{-1}] \times (\cos\theta_{jik} + \frac{1}{3})^2, \quad (2)$$

with $\lambda = 21.0$, $\gamma = 1.20$.

Both f_2 and f_3 vanish if r_{ij} or r_{ik} is greater than a , this being a distance slightly smaller than the second-nearest-neighbor distance 1.83 in the zero-pressure diamond lattice. The three-body part is zero for the diamond lattice because all angles between nearest-neighbor bonds starting from the same atom are tetrahedral, i.e., $\cos\theta = -\frac{1}{3}$. Since the range of f_2 does not include second-nearest neighbors, the distance r_{NN} between nearest neighbors for the diamond lattice under zero pressure is given by the minimum of f_2 , $r_{\text{NN}} = 2^{1/6}$.

Applied to silicon, the unit of length $\sigma = 0.210$ nm, unit of energy $\epsilon = 3.47 \times 10^{-19}$ J, unit of time $t^* = \sigma(m/\epsilon)^{1/2} = 7.66 \times 10^{-14}$ s (m mass of Si atom), and the temperature unit $T^* = \epsilon/k_B = 2.52 \times 10^4$ K. (See Ref. 6 for full details.)

The parameters in the SW potential were chosen so as to make the diamond structure the most stable periodic arrangement of atoms at low pressure. Moreover, the melting point and the liquid structure were sought to be in reasonable agreement with experiment.⁶

The (111) stacking sequence for the diamond lattice is *AaBbCcAa...* Within each plane the atoms are arranged in a triangular lattice with a lattice constant equal to the second-nearest-neighbor distance $\frac{2}{3}\sqrt{6}r_{\text{NN}} = 1.83$. The distance between planes *A-a*, *B-b*, etc. is equal to the nearest-neighbor distance r_{NN} , and the atoms are stacked directly above each other. The distance between planes *a-B*, *b-C*, etc. is $r_{\text{NN}}/3$, atoms of plane *B, C...* being

stacked above the center of the triangles in the lower plane a, b, \dots

It should be mentioned that the SW potential, because of its short-ranged nature, does not distinguish between the diamond and the wurtzite structure ($AaBbAaBb \dots$). The difference in energies between these two structures, however, has been calculated to be much smaller than the difference between diamond and other structures (sc, β -tin, hcp, fcc, and bcc).⁷ Also, one does not expect the SW potential to reproduce the rather complicated 7×7 reconstruction of the Si(111) surface. However, the SW potential properly describes the magic numbers and the topology of ground-state structures of small Si clusters found from quantum-chemistry calculations.⁸⁻¹⁰

Our molecular-dynamics model consists of a Si(111) substrate with three atomic planes at $z = -r_{NN}, 0, \frac{1}{3}r_{NN}$ (stacking sequence AaB). The atoms in the first two layers are fixed at their ideal lattice sites, whereas the atoms in the third layer B are allowed to move as part of the dynamical system. The system is open along the positive z axis, and periodic boundary conditions are applied in the x - y plane which contains the substrate. The x and y dimensions of the simulation cell are adapted to a 14×16 triangular array of atoms. In order to include thermal expansion we make the lattice constant, and by that the x - y cell dimensions, dependent on temperature. For the simulation at higher temperatures we take a lattice constant which is 0.6% larger than the lattice constant at $T=0$. This relatively small value for the thermal expansion agrees with zero-pressure simulations of a SW crystal at higher temperatures.¹¹

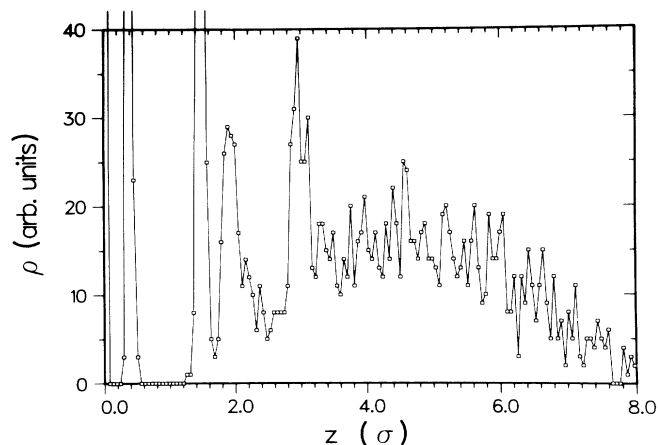


FIG. 1. Density of atoms in the perpendicular z direction to the substrate after the deposition of 1828 atoms at $T_s = 0$.

To simulate the growth process, an atom is introduced every $90\Delta t$ ($\Delta t = 0.02t^*$), moving, at the moment of introduction, perpendicularly towards the substrate. The beam temperature is 40% higher than the melting temperature T_m of the SW model (T_m was determined to be about 0.07).^{12,13} Due to computational limitations, we have to choose a deposition rate which is orders of magnitude higher than the deposition rates usually found in real experiment. Yet, the time between the introduction of atoms in our simulations is comparable to the vibrational

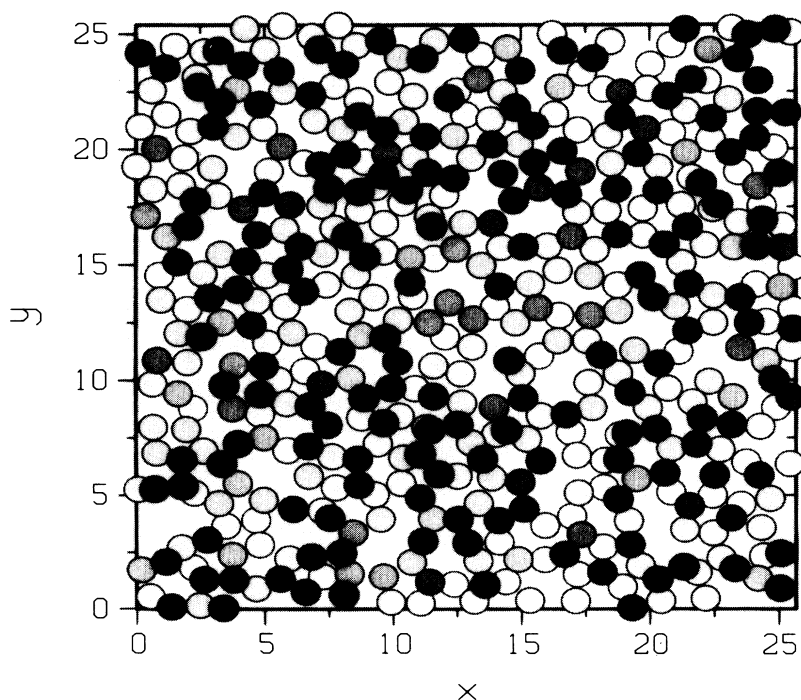


FIG. 2. Atomic arrangement in a horizontal slice of thickness $\Delta z = 1.5$. Different gray values correspond to different z coordinates of atoms.

time of atoms, and most of the atoms approach the adsorbate individually. We think that important short-time relaxations within the system are included in our simulations. Of course, relaxations on a macroscopic time scale cannot be included in such calculations. Since the simulations are rather costly, the influence of the deposition rate on the growth behavior has not been investigated.

The temperature of the adsorbate is controlled via the substrate temperature T_s which in turn is adjusted by periodically scaling the velocities of the atoms in the movable substrate layer. This is an effective procedure to cool the adsorbate to the desired temperature. For the low-temperature simulation with $T_s=0$ the temperature within the adsorbate varies as a function of height z from $T_1=0.004$ in the bottom layers to $T_2=0.012$ in the top layers of the film. In the case of growth at intermediate temperatures the temperature profile ranges from $T_1=0.035$ in the bottom layers to $T_2=0.042$ in the top layers. This temperature of the film surface ($T_2=0.042$) is well below the melting temperature T_m (this can also be seen from the relatively low mobility of the surface atoms in Fig. 5).

The equations of motion are solved numerically with an integration step Δt , and the trajectories of all atoms are followed throughout the simulation as in all standard molecular-dynamics calculations. On a Cray-XMP computer about 68 h CPU time is required to deposit 2500 atoms.

Figure 1 shows the particle density in the z direction, i.e., the direction perpendicular to the substrate, after the deposition of 1828 particles at a temperature $T_s=0$. After the first three layers, i.e., beyond $z=3.0$ in Fig. 1, the atomic distribution is random without any evidence for layered growth. The particle arrangement in the plane of the film shows no evidence for crystallinity; without going into a detailed structural analysis it is appropriate to characterize the structure as being akin to an amorphous material, as shown in Fig. 2. This is opposite to what was

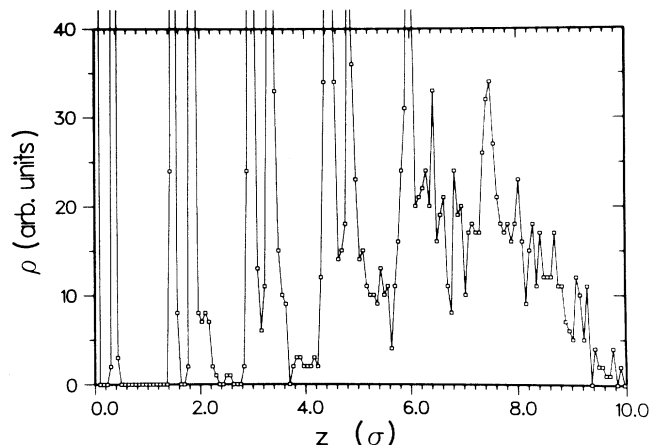


FIG. 3. Atomic density after the deposition of 2492 atoms for a system grown at intermediate temperatures. In order to extract the thermal motion, the system has been cooled to a low temperature without further deposition.

found earlier⁵ using a Lennard-Jones potential where even at the lowest substrate temperatures the growth was into a layered, crystalline structure. Our finding of an amorphous growth for Si at low substrate temperature is in agreement with experimental results which invariably produce an amorphous type of structure.¹⁴ Note the large number of 5–7-membered rings observable in Fig. 2. Long time ($30000\Delta t$) annealing of this structure (at low temperature) did not change these results.

The growth at an intermediate temperature is quite different, as illustrated in Fig. 3 after the deposition of 2492 particles at an adsorbate temperature $T=0.04$. In this case, the growth is into a layered structure as shown in the figure. Note that not only is a layered structure obtained but that the proper stacking distances corresponding to the Si(111) direction persists over 9 layers. The

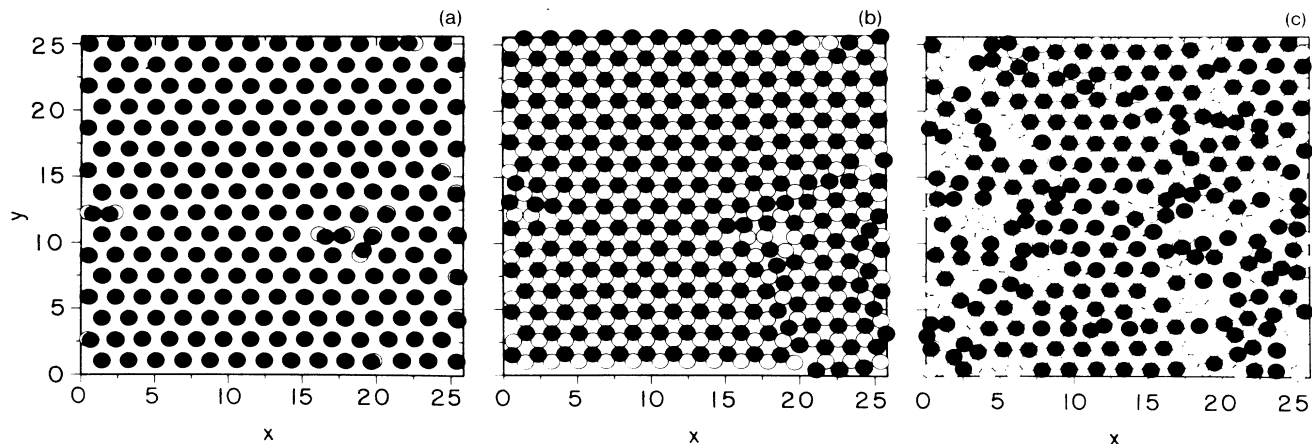


FIG. 4. Atomic arrangements at various heights for the system in Fig. 3. (a) First deposited layer on top of substrate layer (stacking Bb). (b) Second deposited layer on top of first layer (stacking bC and bA). (c) Sixth deposited layer on top of the fifth layer. Figure 4(b) exhibits a grain boundary between two differently stacked regions in the second deposited layer (lower right-hand corner). Such grain boundaries were found to heal at comparable temperatures for the LJ potential.

in-plane structure, however, exhibits some disorder. This is illustrated by an in-plane plot of the atomic positions of two adjacent layers [Fig. 4(a)]. In the perfect single-crystal stacking the atomic positions should be just above each other. The presence of defects is indicated by the fact that in certain areas of the sample, atoms are not perfectly overlapping. At higher levels in the sample more disorder is found, as shown in Figs. 4(b) and 4(c), although large parts of the sample are always found to be well crystallized and are stacked at a proper height. We have observed that the presence of atoms which form overlayers tends to improve the crystallinity of the lower layers. Intuitively this might be expected from a very directional potential such as the one used here.

We recall that in the case of a system of Lennard-Jones particles⁵ a triangular, locally ordered structure was obtained during deposition and the presence of overlayers, as observed here, did not seem necessary to obtain a well-stacked crystal structure.

In order to understand the origin of the differences between the two kinds of simulation, i.e., metallic versus silicon, we have followed the atomic trajectories of particles for $5000\Delta t$ in a vertical slice of the sample (Fig. 5). The figure shows that the atomic mobility in the growing front is somewhat higher than in the bottom layers. A comparison of similar trajectory plots for the Lennard-Jones (LJ) (Fig. 4 of Ref. 5) and the Stillinger-Weber crystals shows that the mobility is much higher in the former (LJ) than in the latter (SW) case. This is probably the reason for the very high order encountered in the LJ growth even without the existence of an overlayer. The physical reason for these differences is perhaps quite easy to understand. A fourfold-coordinated structure is more "rigid" (because of the bond-bending part of the potential) than the structures arising out of the LJ potential, and, therefore, longer times are necessary for the atoms to find their most favorable equilibrium positions.

A comparison with other theoretical and experimental results is quite revealing. Experimental low-energy electron diffraction (LEED) results prove that at low temperatures ($\lesssim 350^\circ\text{C}$) the growth of Si is into an amorphous structure, whereas at intermediate temperatures (600–1100°C) the growth is into epitaxial films.¹⁴ The present calculation is at odds, however, with a Monte Carlo (MC) calculation¹⁵ which claims that the SW potential does not produce growth beyond $\frac{1}{3}$ of a monolayer. Even a

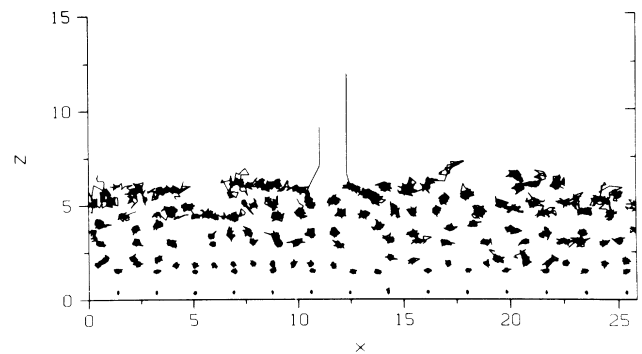


FIG. 5. Trajectory plot at intermediate temperature. A comparison of this figure with Fig. 4 of Ref. 5 clearly shows that the high mobility observed for a LJ potential is not present here.

modification of the potential parameters was suggested as a remedy. A successful crystallization of a disordered SW silicon system has not yet been reported in the literature. In this context one can, in addition, raise questions concerning the efficacy with which escape out of metastable pockets is handled by MC or MD methods, especially when large collective motions in configuration space are needed to obtain the lower-energy minimum. Obviously, the calculations we have presented here cannot give an answer to this difficult question.

In summary, we have studied the vapor-phase growth of silicon using molecular-dynamics techniques and a model potential developed by Stillinger and Weber. At low temperature the system does not show proper stacking and since we have not made a thorough analysis of pair correlations and other properties for a complete characterization we refer to the result as an "amorphouslike" structure; on the other hand, at intermediate temperatures the growth is into well-stacked and properly crystallized structures. The results are in good agreement with experimental results.

This work was sponsored by the U. S. Department of Energy, Basic Energy Sciences Program, Materials Sciences, under Contract No. W-31-109-ENG-38. The calculations were performed on the ER-Cray.

*Deceased.

¹For a review, see, for instance, *Epitaxial Growth*, edited by J. W. Matthews (Academic, New York, 1975).

²See, for instance, J. A. Venables, *Vacuum* **33**, 701 (1983), and references therein.

³H. J. Leamy, G. H. Gilmer, and A. C. Dirks, in *Current Topics in Materials Science*, edited by E. Kaldis (North-Holland, Amsterdam, 1980), Vol. 6, p. 309.

⁴J. Singh and A. Madhukar, *J. Vac. Sci. Technol. B* **1**, 305 (1983).

⁵M. Schneider, A. Rahman, and I. K. Schuller, *Phys. Rev. Lett.* **55**, 604 (1985).

⁶F. H. Stillinger and T. A. Weber, *Phys. Rev. B* **31**, 5262 (1985).

⁷M. T. Yin and M. L. Cohen, *Phys. Rev. B* **26**, 5668 (1982).

⁸E. Blaisten-Barojas and D. Levesque, *Phys. Rev. B* **34**, 3910 (1986).

⁹B. P. Feuston, R. Kalia, and P. Vashishta, *Phys. Rev. B* **35**, 6222 (1987).

¹⁰B. P. Feuston and R. Kalia (private communication).

¹¹J. R. Ray (private communication).

¹²F. F. Abraham and J. Q. Broughton, *Phys. Rev. Lett.* **56**, 734 (1986).

¹³U. Landman *et al.*, *Phys. Rev. Lett.* **56**, 155 (1986).

¹⁴See, for instance, R. N. Thomas and M. H. Francombe, *Appl. Phys. Lett.* **11**, 108 (1967).

¹⁵B. W. Dodson, *Phys. Rev. B* **33**, 7361 (1986).

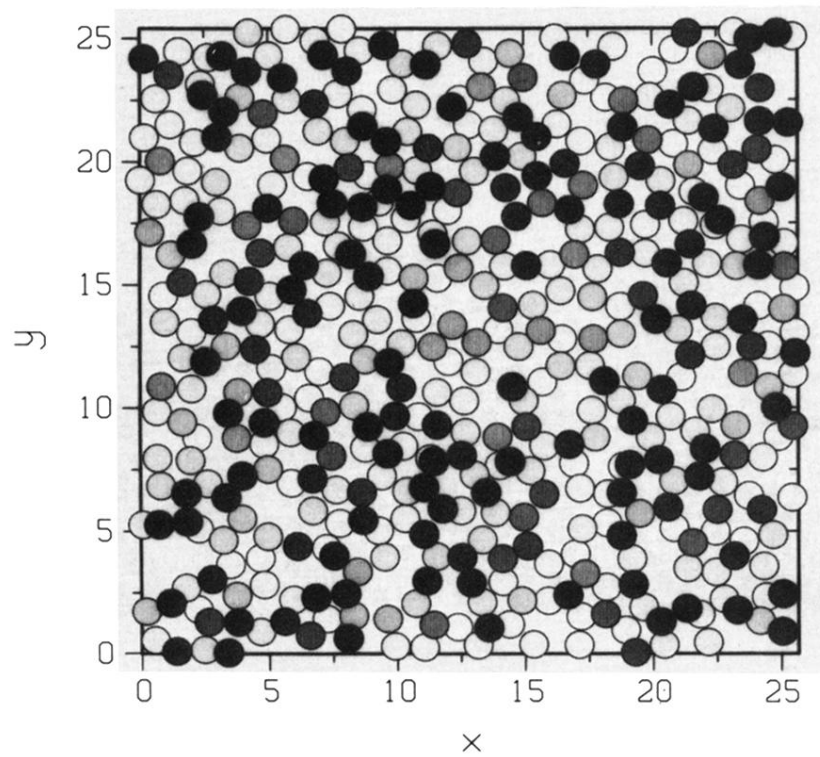


FIG. 2. Atomic arrangement in a horizontal slice of thickness $\Delta z = 1.5$. Different gray values correspond to different z coordinates of atoms.